

The Self-Assembly of a $[\text{Ga}_4\text{L}_6]^{12-}$ Tetrahedral Cluster Thermodynamically Driven by Host–Guest Interactions[†]

Darren W. Johnson and Kenneth N. Raymond*

Department of Chemistry, University of California, Berkeley, California 94720

Received February 27, 2001

The guest-induced synthesis of a $[\text{Ga}_4\text{L}_6]^{12-}$ tetrahedral metal–ligand cluster resulting from a predictive design strategy is described. Each of the six dicatcholamide ligands spans an edge of the molecular tetrahedron with four Ga(III) ions at the vertices. Small cationic species not only were found to occupy the large void volume (ca. 300–400 Å³) inside this cluster but also are necessary thermodynamically to drive cluster assembly via formation of a host–guest complex. NMe_4^+ , NEt_4^+ , and NPr_4^+ all suit this purpose, and in addition the cluster exhibits a preference in the binding of these three guests: NEt_4^+ is bound 300 times more strongly than NPr_4^+ , which is in turn bound 4 times more strongly than NMe_4^+ , as determined by ¹H NMR spectroscopy. The $\text{K}_6(\text{NEt}_4)_6[\text{Ga}_4\text{L}_6]$ cluster was characterized by NMR spectroscopy, high- (Fourier transform ion cyclotron resonance, FT-ICR) and low-resolution electrospray ionization (ESI) mass spectrometry, elemental analysis, and single-crystal X-ray diffraction. The binding of the NEt_4^+ guest molecule was confirmed in the solid state structure, which reveals that the molecule contains large channels in the solid state. As this result exemplifies, it is suggested that guest molecules will play an increasing role in the formation of larger, predesigned metal–ligand clusters.

Introduction

Developing a predictive design strategy for the self-assembly of nanoscale three-dimensional metal–ligand clusters is essential for the rationalization and utility of this area of chemistry.^{1–8} This work has been spurred in part by the desire to utilize the cavities of these molecules as nanoscale reaction vessels^{9,10} and as molecular recognition agents.^{11–13} However, the processes governing the self-assembly of these molecules^{14–16} and the role of the guest molecules in cluster formation are not well understood.

In many cases these three-dimensional supermolecules have cavities large enough for guest encapsulation, but host–guest

interactions do not drive the cluster formation.^{16–25} However, with increasing frequency, guest molecules have been found to play a marked role in cluster formation, either by driving the synthesis of the clusters via host–guest interactions^{18,26–31} or by establishing a guest-mediated equilibrium between multiple clusters.^{32,33} For example, a dicatcholamide ligand assembles

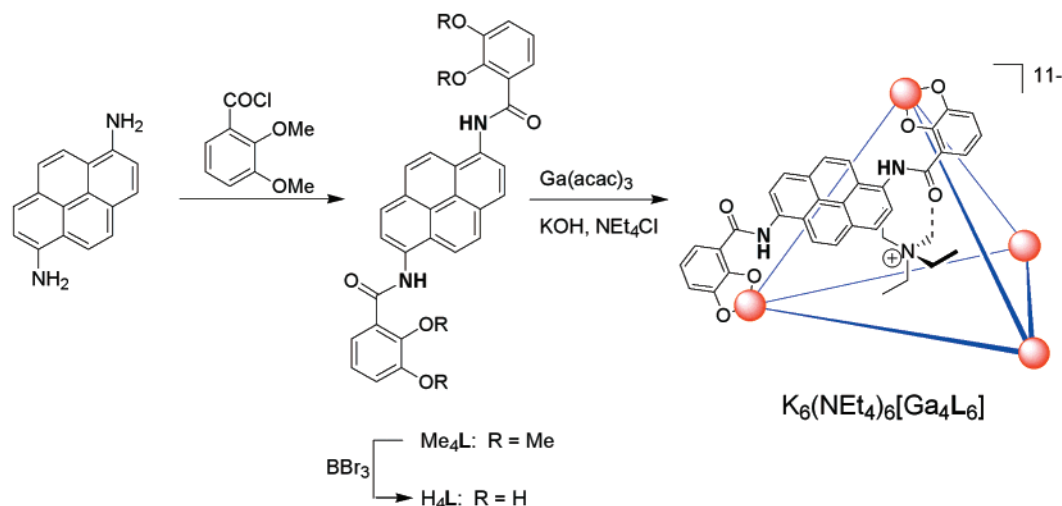
* To whom correspondence should be addressed (e-mail, raymond@socrates.berkeley.edu; url, <http://www.cchem.berkeley.edu/~knrggrp/>).

[†] Coordination Number Incommensurate Cluster Formation. 22. Part 21: Caulder, D. L.; Brückner, C.; Powers, R. E.; König, S.; Parac, T. N.; Leary, J. A.; Raymond, K. N. *J. Am. Chem. Soc.* **2001**, in press.

- (1) Caulder, D. L.; Raymond, K. N. *J. Chem. Soc., Dalton Trans.* **1999**, 1185–1200.
- (2) Caulder, D. L.; Raymond, K. N. *Acc. Chem. Res.* **1999**, *32*, 975–982.
- (3) Leininger, S.; Olenyuk, B.; Stang, P. J. *Chem. Rev.* **2000**, *100*, 853–908.
- (4) Fujita, M. *Chem. Soc. Rev.* **1998**, *27*, 417–425.
- (5) Jones, C. J. *Chem. Soc. Rev.* **1998**, *27*, 289–299.
- (6) Swiegers, G. F.; Malefetse, T. J. *Chem. Rev.* **2000**, *2000*, 3483–3538.
- (7) Saalfrank, R. W.; Bernt, I. *Curr. Opin. Solid State Mater. Sci.* **1998**, *3*, 407–413.
- (8) Saalfrank, R. W.; Demleitner, B. In *Transition Metals in Supramolecular Chemistry*; Sauvage, J.-P., Ed.; Perspectives in Supramolecular Chemistry Vol. 5; John Wiley & Sons Ltd.: Chichester, England, 1999; pp 1–51.
- (9) Yoshizawa, M.; Kusukawa, T.; Fujita, M.; Yamaguchi, K. *J. Am. Chem. Soc.* **2000**, *122*, 6311–6312.
- (10) Ziegler, M.; Brumaghim, J. L.; Raymond, K. N. *Angew. Chem., Int. Ed.* **2000**, *39*, 4119–4121.
- (11) Parac, T. N.; Caulder, D. L.; Raymond, K. N. *J. Am. Chem. Soc.* **1998**, *120*, 8003–8004.
- (12) Aoki, S.; Shiro, M.; Koike, T.; Kimura, E. *J. Am. Chem. Soc.* **2000**, *122*, 576–584.
- (13) Biradha, K.; Aoyagi, M.; Fujita, M. *J. Am. Chem. Soc.* **2000**, *122*, 2397–2398.

- (14) Levin, M. D.; Stang, P. J. *J. Am. Chem. Soc.* **2000**, *122*, 7428–7429.
- (15) Ziegler, M.; Miranda, J.; Andersen, U. N.; Johnson, D. W.; Leary, J. A.; Raymond, K. N. *Angew. Chem.* **2001**, *40*, 733–736.
- (16) Klausmeyer, K. K.; Rauchfuss, T. B.; Wilson, S. R. *Angew. Chem., Int. Ed.* **1998**, *37*, 1694–1696.
- (17) Johnson, D. W.; Xu, J.; Saalfrank, R. W.; Raymond, K. N. *Angew. Chem., Int. Ed.* **1999**, *38*, 2882–2885.
- (18) Saalfrank, R. W.; Burak, R.; Reihls, S.; Löw, N.; Hampel, F.; Stachel, H.-D.; Lentmaier, J.; Peters, K.; Peters, E.-M.; Schnering, H. G. v. *Angew. Chem., Int. Ed. Engl.* **1995**, *34*, 993–995.
- (19) Caulder, D. L.; Powers, R. E.; Parac, T. N.; Raymond, K. N. *Angew. Chem., Int. Ed.* **1998**, *37*, 1840–1843.
- (20) Beissel, T.; Powers, R. E.; Raymond, K. N. *Angew. Chem., Int. Ed. Engl.* **1996**, *35*, 1084–1086.
- (21) Cotton, F. A.; Daniels, L. M.; Lin, C.; Murillo, C. A. *Chem. Commun.* **1999**, 841–842.
- (22) Fujita, M.; Oguro, D.; Miyazawa, M.; Oka, H.; Yamaguchi, K.; Ogura, K. *Nature* **1995**, *378*, 469–471.
- (23) Takeda, N.; Umemoto, K.; Yamaguchi, K.; Fujita, M. *Nature* **1999**, *398*, 794–796.
- (24) Heinrich, J. L.; Berseth, P. A.; Long, J. R. *Chem. Commun.* **1998**, 1231–1232.
- (25) Fox, O. D.; Drew, M. G. B.; Beer, P. D. *Angew. Chem., Int. Ed.* **2000**, *39*, 136–140.
- (26) Sun, X.; Johnson, D. W.; Caulder, D. L.; Powers, R. E.; Raymond, K. N.; Wong, E. H. *Angew. Chem., Int. Ed.* **1999**, *38*, 1303–1307.
- (27) James, S. L.; Mingos, M. P.; White, A. J. P.; Williams, D. J. *Chem. Commun.* **1998**, *21*, 2323–2324.
- (28) Vilar, R.; Mingos, D. M. P.; White, A. J. P.; Williams, D. J. *Angew. Chem., Int. Ed.* **1998**, *37*, 1258–1261.
- (29) Fujita, M.; Nagao, S.; Ogura, K. *J. Am. Chem. Soc.* **1995**, *117*, 1649–1650.
- (30) Aoyagi, M.; Biradha, K.; Fujita, M. *J. Am. Chem. Soc.* **1999**, *121*, 7457–7458.
- (31) Fleming, J. S.; Mann, K. L. V.; Carraz, C.-A.; Psillakis, E.; Jeffery, J. C.; McCleverty, J. A.; Ward, M. D. *Angew. Chem., Int. Ed.* **1998**, *37*, 1279–1281.
- (32) Hiraoka, S.; Fujita, M. *J. Am. Chem. Soc.* **1999**, *121*, 10239–10240.

Scheme 1



an $[\text{M}_2\text{L}_3]^{6-}$ helicate in the absence of a guest; however, the binding of a NMe_4^+ guest cation sways the equilibrium toward an $[\text{M}_4\text{L}_6]^{12-}$ tetrahedron.³³

Often guest molecules have been invoked as templates in the self-assembly of these clusters.^{30,31,34,35} Busch has defined the template effect as either a kinetic or a thermodynamic phenomenon, where “the chemical template organizes an assembly of atoms . . . in order to achieve a particular linking of atoms.”³⁶ In addition, Busch states that the role of the template should not be thought of as a lock-and-key interaction, which resembles a construct in which the key is a constituent part of the assembly. A true template should be removable and leave behind the desired product, as in the case of many macrocycles, catenanes, certain macrobicycles, etc.^{34,37–39} The definition of template as “a pattern, mold, or the like, usually consisting of a thin plate of wood or metal, serving as a gauge or guide in mechanical work” implies that this is a repeatable, i.e., catalytic, process as opposed to a stoichiometric reaction.⁴⁰ Hence one should differentiate between a *thermodynamic* versus *kinetic* template host–guest interaction in metal–ligand cluster formation.³⁶

Here we present the synthesis of a $[\text{Ga}_4\text{L}_6]^{12-}$ tetrahedron derived from a dicatecholamide ligand (H_4L), designed to further elaborate the design strategy for forming tetrahedral clusters.² No discrete cluster forms in the absence of a suitable guest (Scheme 1), but when present the guest molecule *thermodynamically* drives tetrahedral cluster formation and becomes a constituent component of the assembly. ESIMS (electrospray ionization mass spectrometry) data and a single-crystal X-ray diffraction measurement confirm the stoichiometry and connectivity of this cluster and provide another proof of the design principle for forming $[\text{M}_4\text{L}_6]$ tetrahedral clusters.

(33) Scherer, M.; Caulder, D. L.; Johnson, D. W.; Raymond, K. N. *Angew. Chem., Int. Ed.* **1999**, *38*, 1588–1592.

(34) Albrecht, M. J. *Inclusion Phenom. Macrocyclic Chem.* **2000**, *36*, 127–151.

(35) Johnson, D. W.; Raymond, K. N. *Supramolecular Chem.*, in press.

(36) Busch, D. H.; Vance, A. L.; Kolchinski, A. G. In *Templating, Self-Assembly, and Self-Organization*; Sauvage, J.-P., Hosseini, M. W., Eds.; Pergamon: New York, 1996; Vol. 9, pp 1–42.

(37) McMurry, T. J.; Raymond, K. N.; Smith, P. H. *Science* **1989**, *244*, 938–943.

(38) Sauvage, J. P. *Acc. Chem. Res.* **1998**, *31*, 611–619.

(39) Dietrich-Buchecker, C. O.; Khemiss, J.; Sauvage, J.-P. *Chem. Rev.* **1987**, *87*, 795.

(40) *Webster's Encyclopedic Unabridged Dictionary of the English Language*; Gramercy Books: New York/Avanel, NJ, 1989.

Experimental Section

General. All chemicals were used as received from Aldrich. ^1H and ^{13}C NMR data were obtained on a Bruker AM-400 or DRX-500 spectrometer. Mass spectra and elemental analyses were performed at the Elemental Analysis Facility, College of Chemistry, U. C. Berkeley. 1,6-Diaminopyrene was synthesized by a literature protocol and purified from other isomers of the diamine by recrystallization of the dihydrochloride salts from THF/methylene chloride.⁴¹ Abbreviations are as follows: CAM = catecholamide (1,2-dihydroxy-3-carboxamido), MECAM = methyl-protected catecholamide (1,2-dimethoxy-3-carboxamido), \subset signifies that the preceding molecule is a guest of the subsequent species.

1,6-Pyrene-diMECAM (Me_4L). A solution of 2,3-dimethoxybenzoyl chloride (1.38 g, 6.91 mmol) in THF (70 mL) was cooled to 0 °C, as a solution of 1,6-diaminopyrene (0.73 g, 3.14 mmol) and triethylamine (2 mL) in THF was added over 5 min. The yellow solution became cloudy upon addition. This slurry was stirred under nitrogen, as it warmed to room temperature overnight. The inhomogeneous yellow solution was condensed to half volume, and the yellow solid was filtered, taken up in methylene chloride (100 mL), washed with 1 M NaOH (2 × 100 mL) and 1 M HCl (1 × 100 mL), dried, and condensed to a yellow solid (yield 1.33 g, 76%): ^1H NMR (CDCl_3) δ 10.96 (s, 1H, NH), 9.00 (d, $J = 8.4$, 2H, ArH), 8.20 (dd, $J = 8.4$, 2H, ArH), 8.16 (d, $J = 9.2$, 2H, ArH), 8.08 (d, $J = 9.2$), 2H, ArH), 7.91 (d, $J = 7.8$, 2H, catH), 7.26 (t, $J = 7.9$, 2H, catH), 7.15 (d, $J = 8.1$, 2H, catH), 4.15 (s, 3H, OCH₃), 3.99 (s, 3H, OCH₃); FABMS m/z (DTT/DTE) (MH^+) calcd 561, obsd 561; R_f (19:1 CHCl_3 :MeOH) 0.8.

1,6-Pyrene-diCAM (H_4L). To a yellow solution of Me_4L (1.33 g, 2.38 mmol) in CH_2Cl_2 (100 mL) and CHCl_3 (20 mL) cooled to 0 °C under nitrogen was added BBr_3 via a syringe. The cloudy solution was stirred under N_2 for 18 h, as it warmed to room temperature. Volatiles were removed in vacuo, and the resulting yellow solid was taken up in water and heated to boiling. The yellow solid was then filtered and dried (yield 1.15 g, 95%): ^1H NMR (300 MHz, CDCl_3) δ 11.98 (br, 2H, NH), 11.19 (s, 2H, OH), 9.53 (br s, 2H, OH), 8.40–8.38 (m, 4H, ArH), 8.27–8.21 (m, 4H, ArH), 7.70 (d, $J = 8.1$, 2H, catH), 7.05 (d, $J = 7.9$, 2H, catH), 6.86 (t, 2H, $J = 8.0$, catH). The resulting poorly soluble hygroscopic solid was used without further purification in the following reactions.

$\text{NEt}_4\subset[\text{Ga}_4\text{L}_6](\text{NEt}_4)_6\text{K}_6$ Tetrahedron. A solution of H_4L (104 mg, 0.206 mmol), tetraethylammonium chloride (66 mg, 0.40 mmol), and KOH (0.40 mmol as a standardized solution) in MeOH (45 mL) was degassed and stirred under N_2 . (It should be noted that the solution of the poorly soluble H_4L was inhomogeneous until addition of base. The deprotonated ligand and resulting complex have vastly improved

(41) Vollman; Becker; Corell; Streeck. *Justus Liebigs Ann. Chem.* **1937**, *531*, 121.

Table 1. Crystallographic Data

	$\text{NEt}_4\text{C}[\text{Ga}_4\text{L}_6](\text{NEt}_4)_5\text{K}_6 \cdot x(\text{solvent})$
fw	4349.72
cryst syst, lattice	orthorhombic, face-centered
space group	<i>Fdd2</i> (No. 43)
<i>Z</i>	8
<i>a</i> (Å)	46.011(5)
<i>b</i> (Å)	57.883(5)
<i>c</i> (Å)	19.405(2)
<i>V</i> (Å ³)	51681(9)
temp, °C	-96 ± 1
λ , Å	0.71069
μ , cm ⁻¹	5.42
ρ , g cm ⁻³	1.118
R1, wR2 (<i>I</i> > 2 σ (<i>I</i>))	0.1240, 0.3199
R1, wR2 (all data)	0.1658, 0.3549
GOF	1.386

solubilities.) To this yellow solution was added $\text{Ga}(\text{acac})_3$ (49 mg, 0.13 mmol). The solution turned deeper yellow upon addition. This solution was again degassed and stirred under nitrogen for 18 h. The volume of the solution was then reduced to 5 mL, and acetone was added (40 mL) to precipitate a fluffy, yellow solid. This was separated by centrifugation from the yellow filtrate and dried in vacuo: ¹H NMR (400 MHz, $\text{MeOH}-d_4$) δ 14.29 (s, 12H, *NH*), 8.96 (d, *J* = 8.5, 12H, *ArH*), 8.55 (d, *J* = 9.4, 12H, *ArH*), 7.81 (d, *J* = 9.2, 12H, *ArH*), 7.60 (d, *J* = 8.6, 12H, *ArH*), 7.30 (d, *J* = 7.4, 12H, *catH*), 6.68 (d, *J* = 6.8, 12H, *catH*), 6.37 (t, *J* = 7.7, 12H, *catH*), 2.22 (q, 8H, CH_2 exterior), 0.48 (t, 12H, CH_3 exterior), -1.98 (br d, *J* = 34, 8H, CH_2 interior), -3.19 (s, 12H, CH_3 interior); ¹³C{¹H} NMR ($\text{DMSO}-d_6$) δ 229.5, 167.9, 159.3, 158.1, 134.0, 127.6, 125.9, 124.3, 123.6, 120.3, 119.2, 115.2, 113.4, 112.8, 51.7 (exterior NEt_4), 48.4 (interior NEt_4), 7.3 (exterior NEt_4), 1.8 (interior NEt_4); ESIMS *m/z* ($[\text{Ga}_4\text{L}_6]\text{K}_3\text{H}_1(\text{Et}_4\text{N})_4\text{Na}_3^-$) calcd 3990, obsd 3989; FT-ICR ESIMS *m/z* ($[\text{Ga}_4\text{L}_6](\text{Et}_4\text{N})\text{Na}_6^{5-}$) calcd 709.8827, obsd 709.8830, ($[\text{Ga}_4\text{L}_6](\text{Et}_4\text{N})\text{Na}_7^{4-}$) calcd 893.1007, obsd 893.1020. Anal. Calcd for $[\text{Ga}_4\text{L}_6]\text{K}_6(\text{Et}_4\text{N})_6 \cdot 21\text{H}_2\text{O}$: C, 58.56; H, 5.56; N, 5.39. Found: C, 58.38; H, 5.46; N 5.42. X-ray-quality single crystals were obtained by slow vapor diffusion of acetone into a wet DMF solution of the complex.

$\text{Na}_{11}(\text{NPr}_4)[\text{Ga}_4\text{L}_6]$ Tetrahedron (NMR Guest Binding Studies). Reaction was set up in a manner similar to the previous reaction but in an NMR tube using H_4L (10.3 mg, 0.0203 mmol), NMe_4Br (0.523 mg, 0.00339 mmol), $\text{Ga}(\text{NO}_3)_3$ (3.99 mg, 0.0156 mmol), and standardized 15.3 N NaOD solution in D_2O (2.65 μL) dissolved in 2.00 mL of $\text{MeOH}-d_4$ to yield a yellow solution: ¹H NMR (500 MHz, $\text{MeOH}-d_4$ referenced to TMS) δ 8.75 (d, 12H, *ArH*), 8.52 (d, 12H, *ArH*), 7.72 (d, 12H, *ArH*), 7.49 (d, 12H, *ArH*), 7.32 (d, *J* = 7.4, 12H, *catH*), 6.72 (d, 12H, *catH*), 6.39 (t, 12H, *catH*), 1.28 (br, 12H, CH_3). This solution was split up into two 1 mL portions: To one portion was added NPr_4Br (0.45 mg, 0.0017 mmol), and to the other portion was added NEt_4Br (0.28 mg, 0.0017 mmol).

X-ray Diffraction Study of $\text{NEt}_4\text{C}[\text{Ga}_4\text{L}_6](\text{NEt}_4)_5\text{K}_6 \cdot x(\text{solvent})$. Crystal data, details of data collection, structural solution, and refinement are summarized in Table 1. In particular, crystallographic data were collected using a Siemens SMART⁴² diffractometer equipped with a CCD area detector using $\text{Mo K}\alpha$ ($\lambda = 0.71073$ Å) radiation. Data in the frames corresponding to an arbitrary hemisphere of data were integrated using SAINT with a box size of $1.4 \times 1.4 \times 0.5$.⁴³ Data were corrected for Lorentz and polarization effects and were further analyzed using XPREP.⁴⁴ An empirical absorption correction based on the measurement of redundant and equivalent reflections and an ellipsoidal model for the absorption surface was applied using SADABS.⁴⁵ The structure solution and refinement were performed using

SHELXL⁴⁶ (refining on F^2). All oxygen, gallium, and nitrogen atoms of the dodecaanionic cluster and all potassium ions were refined anisotropically, while all other atoms were refined isotropically. Hydrogen atoms were included, but not refined, on all appropriate cluster atoms and the encapsulated tetraethylammonium cation. Due to the low resolution of the structure (1.35 Å, the result of few high-angle data) numerous restraints were employed during structure refinement. All aromatic rings of the cluster were refined as flat rigid groups. One of the two pyrene rings residing on the 2-fold axis of the structure was disordered over two sites. In addition, one molecule of NEt_4^+ was found inside the large cavity of the cluster; however, one of the ethyl groups had to be treated as a rigid group. A large amount of residual electron density was detected in the difference map, attributed to highly disordered solvent and counterions. To account for this, many high-occupancy carbon and oxygen atoms were added, denoted as “*x*(solvent)” in the chemical formula. (It should be noted that only three molecules of NEt_4^+ were found in the difference electron map. The assignment of six NEt_4^+ cations per cluster was derived from elemental analysis and ¹H NMR of the dissolved crystals.) In addition, a solvent–water parameter was utilized to account further for this disordered solvent. Also a rigid-bond restraint and a restraint to refine displacement parameters of neighboring atoms similarly were used. Finally, four low-resolution reflections with $\Delta F/\sigma > 10$ were omitted from the refinement, resulting in a lower *R* value and GOF. Further details are listed in the Supporting Information.

Results and Discussion

Synthesis of Tetrahedral Cluster. Scheme 1 illustrates the synthesis of ligand H_4L from diaminopyrene⁴¹ in a manner similar to that for other previously reported ligands (see Experimental Section).^{47,48} According to our design strategy,^{1,2,19} the antiparallel arrangement of the two catecholate binding groups offset and staggered by a rigid linker (e.g., pyrene) mandates formation of an $[\text{M}_4\text{L}_6]^{12-}$ tetrahedron as the smallest possible discrete species when this ligand self-assembles with a trivalent metal ion. Indeed, from a condensed methanolic solution of $\text{Ga}(\text{acac})_3$, H_4L , KOH, and NEt_4Cl , the desired dodecaanionic tetrahedral cluster precipitates as a yellow solid upon addition of acetone.

NMR spectroscopic data corroborate the existence of a high-symmetry species: one set of resonances for the ligand is observed in both the ¹H and ¹³C{¹H} NMR spectra. These resonances are shifted from that of the free ligand, indicative of metal complex formation. In addition, ¹H resonances at extreme upfield shifted negative δ values for 1 equiv of tetraethylammonium per $[\text{Ga}_4\text{L}_6]$ cluster suggested that this species is encapsulated in the assembly.^{11,33} Integration of the counterion resonances as well as elemental analysis supported the formulation of a $\text{NEt}_4\text{C}[\text{Ga}_4\text{L}_6](\text{NEt}_4)_5\text{K}_6$ cluster. Both low-resolution ESI (electrospray ionization) mass spectrometry (MS) and high-resolution FT-ICR (Fourier transform ion cyclotron resonance) MS of the complex ionized as a methanol solution verified the stoichiometry of the species as $[\text{Ga}_4\text{L}_6]$ (see Experimental Section).

Role of Guest Molecules in Cluster Assembly. To probe the role of the guest in driving this reaction several tetraalkylammonium cations were used in attempts to assemble the tetrahedron. While NMe_4^+ , NEt_4^+ , and NPr_4^+ all allow cluster formation, NBu_4^+ does not; presumably it is too large to suit this purpose. Furthermore, as monitored by ¹H NMR spectroscopy,

(42) SMART, Area Detector Software Package; Siemens Industrial Automation, Inc.: Madison, 1995.

(43) SAINT, SAX Area Detector Integration Program Version 4.024; Siemens Industrial Automation, Inc.: Madison, 1995.

(44) Sheldrick, G.; SHELXL.; Siemens Industrial Automation, Inc.: Madison, 1993.

(45) Sheldrick, G.; SADABS, Siemens Area Detector ABSorption Correction Program; Personal Communication, 1996.

(46) Sheldrick, G.; SHELXL Version 5.1 Crystal Structure Determination Software Package; Siemens Industrial Automation, Inc.: Madison, 1998.

(47) Caulder, D. L.; Raymond, K. N. *Angew. Chem., Int. Ed. Engl.* **1997**, *36*, 1439–1442.

(48) Meyer, M.; Kersting, B.; Powers, R. E.; Raymond, K. N. *Inorg. Chem.* **1997**, *36*, 5179–5191.

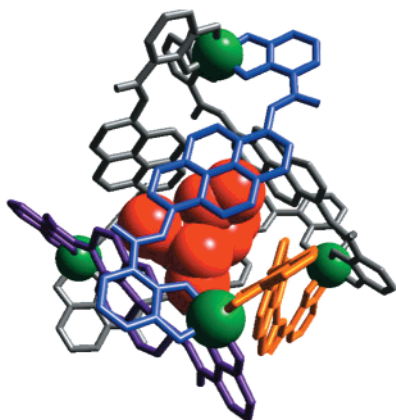
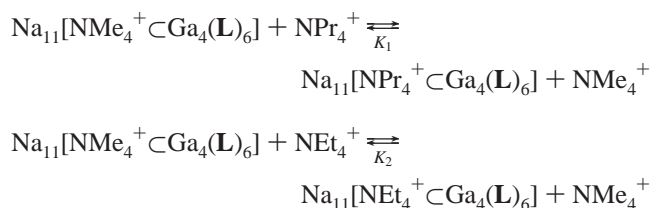


Figure 1. The solid state structure of the $\text{NEt}_4^+[\text{Ga}_4\text{L}_6]^{11-}$ tetrahedron. The view depicts the tetrahedron sitting on one of the cluster's tetrahedral faces. For clarity the ligands are represented as wireframes, with the front three ligands blue, purple, and gold and the back three ligands gray; the gallium ions are green spheres, and the guest is shown as a red space-filling model.

copy in $\text{MeOH-}d_4$, competition experiments revealed that NPr_4^+ displaces NMe_4^+ from the cluster cavity, which in turn is displaced by NEt_4^+ . Efforts at removing the guest from the cluster have failed, barring the complete destruction of the cluster at acidic pH. That the cluster does not form in the absence of one of these guests, even using longer reaction times in refluxing DMF solutions, provides further evidence that the guest thermodynamically drives cluster formation. This suggests that our design strategy still holds for these large molecules, but as the cluster volume increases, the binding of guest molecules may be needed to thermodynamically drive cluster assembly.

Relative binding constants were also determined by a ^1H NMR spectroscopic experiment. On an NMR tube scale two separate batches of $\text{Na}_{11}(\text{NMe}_4)[\text{Ga}_4\text{L}_6]$ were prepared in $\text{MeOH-}d_4$, and their spectra were recorded (see Experimental Section). To one sample was added 1 equiv per tetrahedron of NEt_4Cl . To the other sample was added 1 equiv of NPr_4Br . Both of these new solutions were allowed to equilibrate over the course of 4 h, and their ^1H NMR spectra were again recorded. Integration of the signals corresponding to the tetralkylammonium species provided equilibrium concentrations, and thus a relative value for the respective K_{eq} 's could be determined for the two processes according to the following equilibria:



From this experiment it was determined that NEt_4^+ was bound 300 times more strongly than NMe_4^+ and NPr_4^+ was bound 4 times more strongly than NMe_4^+ (i.e., $K_1 = 4$, $K_2 = 300$). This compares well with values previously determined for this type of guest in similar tetrahedral clusters.^{11,49}

X-ray Structural Study of Tetrahedral Cluster. A single-crystal X-ray structure of $\text{K}_6(\text{NEt}_4)_6[\text{Ga}_4\text{L}_6] \cdot \text{MeOH} \cdot 4\text{H}_2\text{O}$

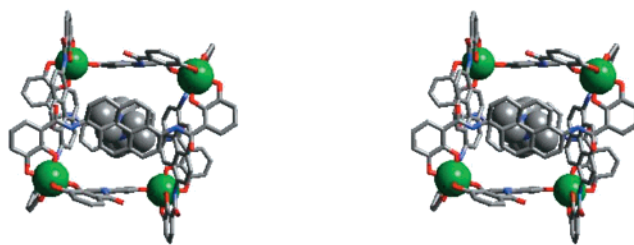


Figure 2. A stereo representation of the crystal structure of $\text{NEt}_4^+[\text{Ga}_4\text{L}_6]^{11-}$ as viewed down the crystallographic 2-fold axis. The ligand is represented as a wireframe with carbon atoms gray, oxygen atoms red, and nitrogen atoms blue. The gallium ions are green spheres, and the guest is a space-filling model.

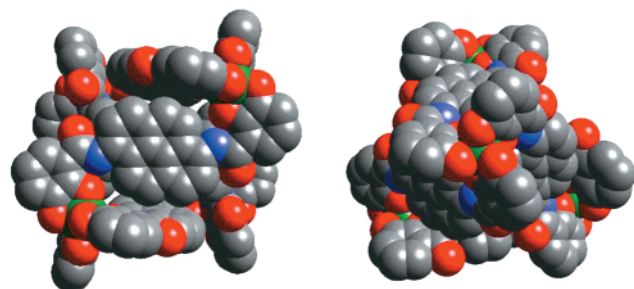


Figure 3. A space-filling representation of the crystal structure of $\text{NEt}_4^+[\text{Ga}_4\text{L}_6]^{11-}$ viewed down the crystallographic 2-fold axis (left) and pseudo-3-fold axis (right). The same color scheme as in Figure 2 is used.

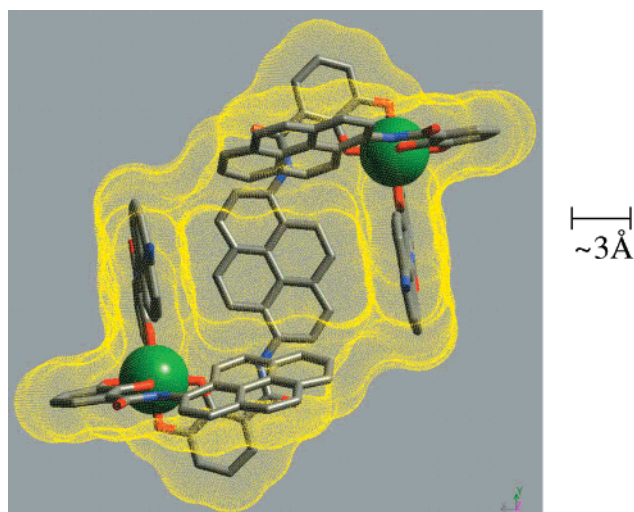


Figure 4. A slice through the center of the tetrahedron shows the environment of the guest in the Ga_4L_6 host. The ligands are represented as wireframes with the same color scheme as used in Figure 2. The yellow dots around the ligands are a representation of their space-filling surfaces, which is slightly smaller than the van der Waals radii.

$x(\text{solvent})$ (Figure 1) unambiguously verifies the guest inclusion, stoichiometry, and connectivity of this cluster in the solid state (cf. Experimental Section, Supporting Information, and Table 1). The molecule crystallizes out of a wet DMF/acetone solution in orthorhombic space group $Fdd2$ with $Z = 8$. In addition, the cluster exists as a racemic mixture of homoconfigurational tetrahedra (i.e., within one molecule the metal centers all have either Δ or Λ configurations).

The molecule has 2-fold crystallographic symmetry with the four gallium ions at the vertices and the ligands comprising the edges of a slightly distorted tetrahedron (Figure 2). The average Ga–Ga distance is 14.31 Å with a range of 14.13–14.45 Å.

(49) Note that these spectra did not change over the course of several days. In addition, the error in this experiment is roughly 15% and results from errors in measuring precise amounts of compound and integration of the signals in the NMR spectra.

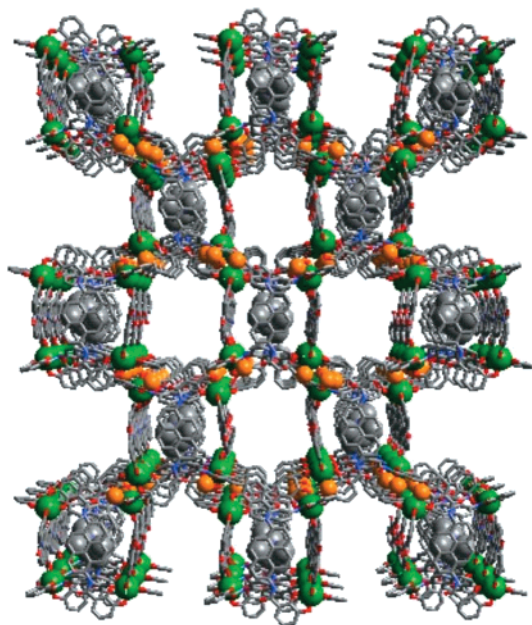


Figure 5. Extended solid state structure of $\text{NEt}_4^+[\text{Ga}_4\text{L}_6]^{12-}\text{K}_6^{5-}$. The same color scheme as in Figure 1 is used with potassium ions represented as orange spheres. The height and width of the figure are slightly over one unit cell length, and the depth is three unit cell lengths (58.2 Å).

As expected from the NMR data, one molecule of NEt_4^+ was found incarcerated within the box-like cluster cavity. The space-filling model of the solid state structure shows that this guest is completely sequestered from its surroundings by the extended π -system of the pyrene rings (Figure 3). This suggests a cavity size of ca. 300–400 Å³, slightly larger than previously reported for a cluster with a naphthyl linker in the ligand.^{19,50}

The ligand distortion within the tetrahedron varies greatly; the angle between the planes of the catecholates and the pyrene rings ranges from 0.8° to 46.0° with an average of 23°, probably a result of the asymmetric guest encapsulated in the cluster cavity. Pictured in Figure 4 is a slice through the center of the tetrahedron with the guest removed showing the environment within the cavity.⁵¹ The ligand is illustrated as a wireframe with its space-filling surface represented as yellow dots. It is apparent from this illustration that the environment the guest “sees” within the cavity is much like that of liquid pyrene. The six pyrene moieties have distorted from a true octahedron around the ethyl arms of the guest in order to make van der Waals contact with the guest. In addition, the chirality at the metal centers is not transferred to the cavity in any way, which explains why no selectivity has been observed in the binding of various chiral guests.

Further analysis of the structure reveals a pleasant surprise, one never observed before in crystal structures of supramol-

ecules from this group, and rarely seen in the literature for supramolecular metal–ligand clusters:^{3,52} The three-dimensional packing of this molecule shows remarkably large channels running entirely through the crystal lattice in the *c*-direction (Figure 5). These channels are roughly 15 Å square, as measured from the center of one pyrene ring across the channel to the center of an opposite pyrene ring. In these channels much disordered solvent was found in the difference map, some of which is coordinated to the potassium ions that hold this 3-D structure together. At each vertex of the tetrahedral anion, three potassium ions link each cluster to an adjacent one. This forms a quaternary structure: the ligand is the primary structure; the interaction with one metal ion is the secondary; the self-assembly of the tetrahedron is the tertiary structure; and these interactions with the potassium counterions generate the quaternary structure. This description is analogous to those of the extended structures of proteins.

In summary, the synthesis of a metal–ligand tetrahedron *thermodynamically* is driven by a host–guest interaction. This exemplifies our design strategy for forming tetrahedral clusters and begins to elucidate the role of the guest molecule in cluster formation.

Acknowledgment. We thank the National Science Foundation (CHE-9709621) and NSF/NATO (Exchange Grant INT-9603212/SRG951516) for financial support. The authors also thank Dr. Dana L. Caulder for assistance with the X-ray crystal structure solution and for helpful discussions. In addition we wish to thank Dr. Stefan Koenig and Prof. Julie A. Leary for obtaining low-resolution ESIMS data and J. J. Miranda, Dr. Marco Ziegler, Dr. Ulla N. Andersen, and Prof. Julie A. Leary for obtaining high-resolution FT-ICR ESIMS data. The FT-ICR mass spectral data were collected in the Chemistry Department’s Mass Spectrometry Facility and funded by NSF grant CHE-9870989. The cover artwork was prepared using the Weblab Viewer and Pov-Ray software packages, and the authors thank Fraser Hof for assistance in preparing the picture.

Note Added after ASAP. The Acknowledgment that appeared in the version of this article posted on July 14, 2001, was incomplete. The complete Acknowledgment appears in the version posted on September 17, 2001.

Supporting Information Available: Crystallographic data in CIF format. This material is available free of charge via the Internet at <http://pubs.acs.org>. In addition, listings of crystallographic data (excluding structure factors) have been deposited with the Cambridge Crystallographic Data Centre as supplementary publication number CCDC 144536. Copies of the data can be obtained free of charge on application to The Director, CCDC, 12 Union Road, Cambridge CB21EZ, UK (fax, int. code + (1223)336-033; e-mail, deposit@chemcrs.cam.ac.uk).

IC0102283

(50) This is based on the longer metal–metal distances (12.8 Å for the naphthyl-based cluster versus 14.3 Å for $[\text{Ga}_4\text{L}_6]$), the expanded size of pyrene versus naphthalene, and CAChe (MM3) molecular models. To our surprise, this has little bearing on guest encapsulation preference (see text).

(51) *Cerius2 Version 3.5*; Molecular Simulations, Inc.: San Diego, 1997.

(52) For several representative examples of X-ray structures of metal–ligand supramolecular clusters possessing channels, see: (a) Stang, P. J.; Cao, D. H.; Saito, S.; Arif, A. M. *J. Am. Chem. Soc.* **1995**, *117*, 6273–6283. (b) Cotton, F. A.; Chun, L.; Murillo, C. A. *Inorg. Chem.* **2001**, *40*, 478–484.